

# Simulation of a Hydrometallurgical Leaching Reactor modeled as a DAE system

Dueñas Díez M., Ausland G.\*\* , Fjeld M.\*\*\* & Lie B.\*

Telemark University College

Department of Automation

P.O. Box 203, N-3901, Porsgrunn, Norway

\*\*Elkem Research Centre

P.O. Box 8040, Vaagsbygd, N-4675 Kristiansand, Norway

\*\*\* Fjeld Consulting

Meltzers gt. 4, N-0257, Oslo, Norway

## Abstract

An existing dynamic model of the main reactor in the Silgrain<sup>®</sup> process for the production of Si from FeSi has been extended here in order to resemble more closely the behavior of the real reactor. The previous model was based on the application of macroscopic mass conservation law, the population balance equation and the assumptions of complete mixing and isothermic conditions. The major modifications are the inclusion of the condition governing the entrainment of particles in the outflow, and the formulation of the energy balance.

The extended model consists of 1 integrodifferential equation, 4 implicit ordinary differential equations, 7 algebraic equations and 3 integral equations. After discretization in the particle size space, a system of differential and algebraic equations (DAE) is obtained. DAEs are not ODEs and they require analysis and characterization and may require reformulation. After such analysis, it was concluded that the system is implicit index-one for the usual range of operation and that a method based on the Backward Differentiation formulas (BDF) can be used for its solution.

The model was implemented in MATLAB and the `ode15s` code was used for solving the system of equations. The simulation results are satisfactory and seem to match qualitatively with the known operation of the reactor. The model is suitable for further use in designing a model-based control scheme.

**Keywords:** Population Balance Equation, Differential and Algebraic Equations, leaching, dynamic modeling, ferrosilicon

## 1 Introduction

Silicon (Si) is one of the most important technical materials due to its properties as semiconductor. Elkem Bremanger at Svelgen (Norway) produces Si metal via a patented hy-

---

\*Author to whom correspondance should be adressed.

drometallurgical leaching process called the Silgrain<sup>®</sup> process. Hydrometallurgical leaching belongs to the category of reactive particulate processes, which are inherently more difficult to describe than reactive systems comprised of one or more bulk phases, due to the fact that dispersed particles in liquid phase are invariably polydispersed in nature.

A model of the leaching reactor in the Silgrain process was developed in (Dueñas & Lie 2000) to simulate the dynamic response of the main reactor in the process. This model was based on the application of the macroscopic mass conservation law, the Population Balance Equation (PBE) and the assumptions of complete mixing and isothermic conditions. The PBE is the most suitable approach to build dynamic models of particulate processes since it accounts for the polydispersed nature of such processes. This model accounted for the main event taking place within the reactor: the disintegration of particles, but it could not represent properly the practical operation of the reactor.

The model of the hydrometallurgical leaching reactor has been reviewed recently, and extended to resemble more closely the operation of the reactor. The main modification is the inclusion of the condition governing the entrainment of particles in the outflow, thus permitting a distinction between the particle size distribution (PSD) of the outflow and the PSD within the reactor, as it happens in reality. Another major change is the formulation of the energy balance that was necessary since temperature has an important influence on the operation of the reactor.

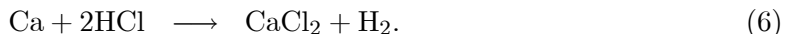
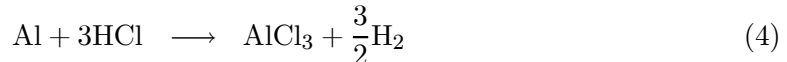
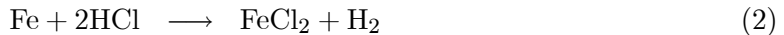
The resulting mathematical model is highly nonlinear and is composed of one partial integro-differential equation, ordinary differential equations and algebraic equations. Such a system is difficult to solve. The solution of the model is approached by discretizing the PBE in the particle size space, which reformulates the system into a system of Differential and Algebraic Equations (DAE). Historically, sets of DAEs were frequently reformulated and solved as ODEs, by differentiation and/or extensive algebraic manipulation. However, it is advantageous to keep the system in the DAE form, mainly because the variables have a physical significance that is lost when reformulating the DAEs to ODEs. However, DAEs are not ODEs and difficulties can be encountered when using numerical methods to solve DAEs (Petzold 1985). DAEs are solvable by numerical methods provided they are low index and consistent initial conditions are given. Thus, DAEs require analysis and characterization and may require reformulation before approaching its numerical solution.

The paper is organized as follows: In section 2, we give a brief description of the operation of the reactor in the Silgrain<sup>®</sup> process. In section 3 the model is discussed in detail, section 4 shows the analysis of the DAE system which results from the modeling stage and suggests the method to be used for the solution of the system. Section 5 presents some simulation results, and finally the conclusions are presented in section 6.

## 2 Operation of the reactor

Leaching is the dissolution of a soluble constituent from a solid by means of a solvent. Aas (1971) described the process of hydrometallurgical leaching of ferrosilicon in detail. Silicon metal is produced by leaching lumps of 90 – 94% FeSi in a hot acidic solution of ferric chloride and hydrochloric acid. The acid dissolves the impurities, mainly Fe, Al and Ca, breaking apart the lumps and leading to a granulated product of high purity (Si). The dissolution of impurities is assumed to proceed according to the following reduction-

oxidation equations (Aas 1971), (Margarido, Martins, Figueiredo & Bastos 1993):



One feature that characterizes the Silgrain<sup>®</sup> Process and distinguishes it from other hydrometallurgical leaching processes is the rapid disintegration of FeSi into small grains during the reaction (Aas 1971).

A simplified sketch of the reactor is shown in Figure 1. The hot acidic solution is continuously pumped into the bottom of the vertical reactor and it leaves the reactor through an overflow pipe near the top, together with the disintegrated product. FeSi lumps are fed on the top of the reactor and sink to the bottom. The contact of the lumps with the hot acid causes the disintegration of the lumps, and the smallest grains are displaced upwards by the acid upflow (Aas 1971).

The high flowrate of acid and the gas evolved during leaching causes agitation within the reactor, but gravity classification of the solid charge still occurs. The upper layers consist of the fine particles that are displaced by the upward flow, whereas the deeper layers consist of unreacted and partially-reacted lumps of FeSi.

Clearly the assumption of complete mixing is not realistic, since only the disintegrated material that is small enough to be displaced by the acid upflow, flows out of the reactor. This means that the particle size distribution at the outlet differs from the particle size distribution within the reactor.

Aas (1971) stresses the importance of operating with FeSi lumps of the right composition, as well as using the right type of leach liquor. Temperature and leaching time play also an important role. This means that it is important to include the energy balance in the model.

### 3 Model

The reactor is modeled as one well-mixed reaction region and one well-mixed storage region in series. Figure 2 shows a sketch of the suggested model.

The residence time in the upper layers of the reactor, a mixture of acid and fine particles, is much shorter than the residence time in the bottom part. Therefore, it is reasonable to assume that no disintegration or reaction occur in the upper part of the reactor, so we can model it as a storage tank. Moreover, the FeSi lumps sink quickly through the upper layers, and do not accumulate there, so that it can be assumed that the feed enters directly into the well-mixed reaction region.

The high acid flowrate and the generation of gas during the reactions ensures agitation and well mixing conditions in both regions. Although we can assume homogeneity conditions within the reaction region, the particle size distribution of particles leaving it

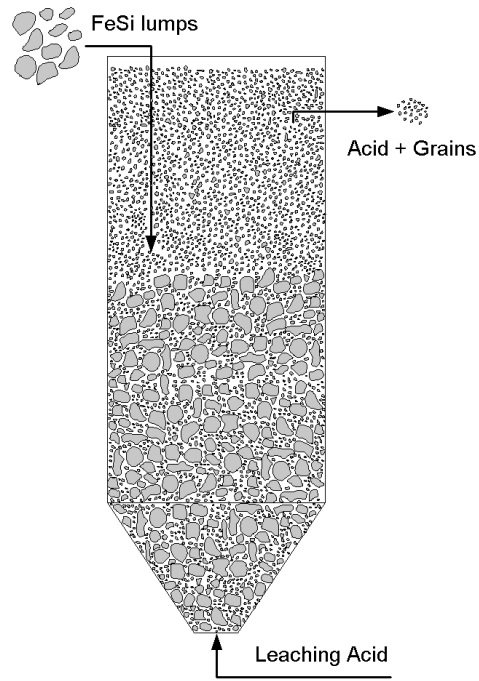


Figure 1: Main Reactor in Silgrain Process.

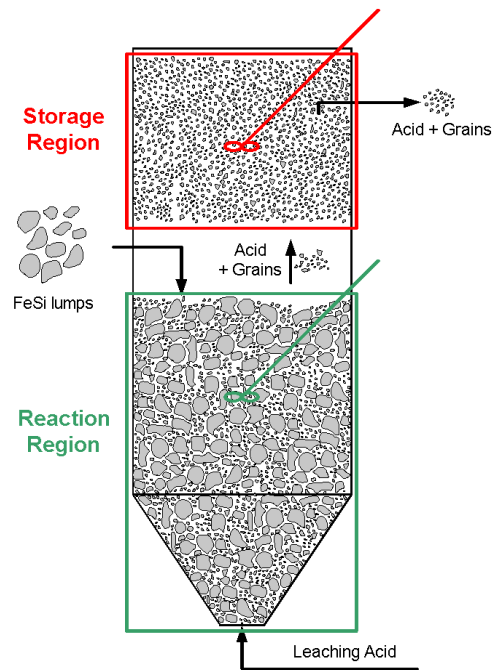


Figure 2: Model of Silgrain main reactor.

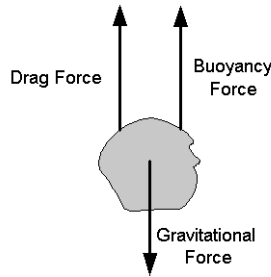


Figure 3: Forces acting on a particle.

is not the same as the particle size distribution of the particles remaining in that region. The free-falling velocity of the particles is the factor that determines whether the particles remain in the bottom part or flow up with the acid. As shown in Figure 3, each particle is subjected to three forces: the gravitational force, the drag force and the buoyancy force. For a certain particle diameter, to which we will refer as cut-size, the free-falling velocity equals the velocity of the upflow acid. Particles smaller than that cut size are displaced by the upflow, and particles larger than the cut size are not displaced.

The model suggested here consists in the application of:

- the PBE to the reaction region and to the storage region.
- the mass conservation law to the reaction region and to the storage region.
- the energy balance to the whole reactor.

All of these are discussed in more detail in the following sections.

### 3.1 Population Balance Equation

In 1964, two groups of researchers, Hulburt & Katz (1964) and Randolph (1964), observed that many problems involving change in particulate systems could not be handled within the framework of the conventional conservation equations. These researchers recognized that particulate materials are unique in that the dispersed phase is made up of a countable number of entities, and these entities possess a distribution of properties. They proposed the use of an equation for the continuity of particulate numbers, termed *population balance*, as a basis for describing the behavior of such systems. This number balance is developed from the general conservation equation

$$\text{accumulation} = \text{input} - \text{output} + \text{net generation}$$

applied to particles having a specified set of properties. In the population balance, input and output terms represent changes in the number of particles in the specified property interval due to convective flow, while the net generation term accounts for particles entering and leaving the specified property intervals as a result of continuous processes such as chemical reaction, or discrete generation such as particle breakage.

Originally derived for the study of crystal nucleation and growth (Randolph 1964) (Hulburt & Katz 1964), the population balance has since then proven to be a powerful tool for quantifying the dynamics of many varied particle technologies such as crushing, agglomeration, liquid-liquid extraction, biochemical processes, emulsion polymerization, etc. Randolph and Larson (1988) and Ramkrishna (1985) present a complete review of the application of population balances to problems in chemical engineering. This approach was first applied to hydrometallurgical leaching in single steady-state reactors by Herbst (1971). Rubisov and Papangelakis (1995, 1996a, 1996b) were the first to successfully model the transient behaviour of hydrometallurgical leaching reactors.

In the field of reactive particulate processes, the macroscopic version of the PBE is commonly used

$$\frac{d\psi(D_p, t)}{dt} + \frac{\psi(D_p, t)}{V(t)} \frac{dV(t)}{dt} = \frac{1}{V(t)} \left( \sum_i q_{in,i}(t) \psi_{in,i}(D_p, t) - \sum_i q_{out,i}(t) \psi_{out,i}(D_p, t) \right) - \frac{\partial}{\partial D_p} \left( \frac{dD_p}{dt} \psi(D_p, t) \right) + B - D \quad (7)$$

where  $\psi(D_p, t)$  ( $\text{m}^{-4}$ ) is the number-density particle size distribution function *per unit working volume* and only one distributed property, the particle diameter  $D_p$ , is considered. The left hand side of equation 7 is the accumulation term, where  $V(t)$  represents the working volume of the reactor ( $\text{m}^3$ ), which is a function of time. The first two terms of the right hand side of equation 7 represent the input and output by convective transport, where  $Q_{in}(t)$  and  $Q(t)$  are the slurry flow rate ( $\text{m}^3/\text{min}$ ) at the inlet and outlet, respectively. The generation term consists of two parts: a continuous disappearance of particles,  $\frac{\partial}{\partial D_p} \left( \frac{dD_p}{dt} \psi(D_p, t) \right)$  and a discrete generation of particles represented by the birth and death of particles by disintegration (the last two terms of the right hand side).

In the reactive region of the Silgrain reactor the two main events taking place are: disintegration of the particles and convective transport, and therefore, the population balance reduces to:

$$\frac{d\psi_1(D_p, t)}{dt} + \frac{\psi_1(D_p, t)}{V_1(t)} \frac{dV_1(t)}{dt} = \frac{1}{V_1(t)} \left( \dot{M}_{in}(t) f_{in}(D_p, t) - q_{inter}(t) \psi_{inter}(D_p, t) \right) + B - D \quad (8)$$

where  $\dot{M}_{in}(t)$  is the mass input of FeSi ( $\text{kg}/\text{min}$ ),  $f_{in}(D_p, t)$  is the PSD of the FeSi expressed as weight-based probability distribution function ( $\text{m}^{-1}$ ),  $V_1(t)$  is the volume of the reaction region,  $\psi_1(D_p, t)$  is the PSD function per unit working volume within the reaction region,  $\psi_{inter}(D_p, t)$  is the PSD leaving the reaction region and entering the storage region,  $B$  represents the birth of particles of size  $D_p$  resulting from breakage of larger particles and the  $D$  represents the disappearance of particles of size  $D_p$  due to disintegration. Let us discuss some of the terms in more detail.

1. The relationship between  $\psi_1(D_p, t)$  and  $\psi_{inter}(D_p, t)$  is given by the balance of forces acting on the particles. As discussed earlier, particles larger than the cut size remain in the reaction region and particles smaller than the cut size are displaced by the upflowing acid. Assuming that fines are displaced in the same concentration as within

the reactor, the relationship of the two particle size distributions can be written as follows:

$$\psi_{\text{inter}}(D_p, t) = \begin{cases} \psi_1(D_p, t) & \text{for } D_p \leq D_{\text{cut}} \\ 0 & \text{for } D_p > D_{\text{cut}} \end{cases} . \quad (9)$$

The cut size can be obtained from the balance of forces on the particle

$$\text{Drag Force} = \text{Gravity Force} - \text{Buoyancy Force}$$

and if we assume the particles are spherical (Coulson & Richardson 1978)

$$R_o \frac{\pi}{4} D_{\text{cut}}^2 = \frac{\pi}{6} D_{\text{cut}}^3 \rho_p g_r - \frac{\pi}{6} D_{\text{cut}}^3 \rho_f g_r, \quad (10)$$

where  $R_o$  is the dimensionless drag force,  $\rho_p$  and  $\rho_f$  are the solid density and the fluid density, respectively, and  $g_r$  is the gravity constant. The drag force is generally a complicated function of the Reynolds number  $Re$ , but for turbulent flow ( $500 < Re < 2 \cdot 10^5$ ), as in the reactor under study, the drag force is independent of the Reynolds number (Coulson & Richardson 1978)

$$\frac{R_o}{\rho_f u_0^2} = 0.22, \quad (11)$$

where  $u_0$  is the fluid velocity. Substituting 11 into equation 10 gives

$$D_{\text{cut}} = 0.33 \frac{\rho_f}{g_r (\rho_p - \rho_f)} u_0^2 \quad (12)$$

$$= 0.33 \frac{\rho_f}{g_r (\rho_p - \rho_f)} \left( \frac{u_{et}}{(1 - g_2)^n} \right)^2, \quad (13)$$

where the fluid velocity has been expressed as a function of the the superficial fluid velocity  $u_{et}$  and the porosity  $(1 - g_1)$  in the storage region.

2. The discrete generation of particles in a certain particle diameter range is the result of the disintegration process. Such an event is typically represented by the particle birth and particle death rates,  $B$  and  $D$ , respectively. No references have been found of the application of the PBE to leaching processes where the particles experienced disintegration. However, numerous references have been found of the application of PBE that include the birth and death rate functions in other fields of particulate processing such as granulation (Kapur 1995), comminution (Herbst & Asihene 1993), (Ramkrishna 1985), and emulsion dispersion (Chen, Prüss & Warbecke 1998). It is important to note that although these particulate processes differ considerably, they model the birth and death rate terms in an identical way, as follows:

$$B - D = \int_{D_p}^{\infty} b(D_p, y) a(y) \eta(D_p, y) \psi_1(y, t) dy - a(D_p) \psi_1(D_p, t) \quad (14)$$

where  $a(D_p)$  is the particle breakup frequency function ( $\text{min}^{-1}$ ),  $b(D_p, y)$  is the probability distribution function of daughter particles of size  $D_p$  by breakage of a particle of size  $y$ , and  $\eta(D_p, y)$  is the average number of daughter particles by

breakage of one particle of size  $y$ . Such a mathematical formulation for the discrete generation is used here. Batch laboratory experiments have been carried out to determine expressions for the particle breakup frequency function and the probability distribution function. The particle breakup frequency function depends mainly on the particle size and temperature and when particles are as small as the average grain size they do not disintegrate anymore. We thus propose the following expression

$$a(D_p, T) = \begin{cases} \frac{k_a \exp(k_T T)}{D_p^n} & \text{for } D_p \leq D_{\text{grain}} \\ 0 & \text{for } D_p > D_{\text{grain}} \end{cases} \quad (15)$$

for the particle breakup frequency function, where  $k_a$ ,  $k_T$  and  $n$  are the fitting parameters and  $D_{\text{grain}}$  depends on the quality of the feed material used in the process. Regarding the probability distribution function of daughter particles, the laboratory results showed a bimodal distribution function, in which one of the modes is static at a certain particle size diameter  $D_p^*$  and the other one depends on the size of the mother particle  $y$ . The distribution functions commonly encountered in the references did not fit the data well. We suggest then the following expression:

$$b(D_p, y) = A_1 \exp\left(-\beta_1 \left(1 - \frac{D_p}{D_p^*}\right)^2\right) + \frac{A_2}{D_p} \exp\left(-\beta_2 \log^2\left(1 - \frac{D_p y}{(y - D_p) D_p^*}\right)\right), \quad (16)$$

which shows good fitting properties to the experimental data, and where  $A_1$ ,  $\beta_1$ ,  $A_2$ ,  $\beta_2$  and  $D_p^*$  are the fitting parameters. Finally, the average number of daughter particles  $\eta(D_p, y)$  by breakage of one particle of size  $y$  can be obtained from the dimensional analysis of equation 14. The suggested expressions have the following dimensions:  $b(D_p, y)$  gives the mass of particles of size  $D_p$  obtained per unit mass of mother particle of size  $y$  that experiences breakage,  $\psi_1(y, t)$  gives the number of mother particles of size  $y$  per unit working volume,  $a(y, T)$  gives the rate of breakup of a mother particle of size  $y$  and  $B$  is the number of particles of size  $D_p$  that are created per unit time and per unit working volume. Therefore, in order to match dimensions,  $\eta(D_p, y)$  is the ratio between the mass of one mother particle and the mass of one daughter particle

$$\eta(D_p, y) = \frac{\rho_p \pi / 6 y^3}{\rho_p \pi / 6 D_p^3} = \frac{y^3}{D_p^3}. \quad (17)$$

In the storage region of the Silgrain reactor the main event taking place is the convective transport, and therefore, the population balance reduces to:

$$\frac{d\psi_2(D_p, t)}{dt} + \frac{\psi_2(D_p, t)}{V_2(t)} \frac{dV_2(t)}{dt} = \frac{1}{V_2(t)} (q_{\text{inter}}(t) \psi_{\text{inter}}(D_p, t) - q_{\text{out},2}(t) \psi_2(D_p, t)) \quad (18)$$

where the inlet flow is equal to the outlet flow from the reaction region and where the PSD within the storage region is the same as the PSD in the outlet flow since the assumption of complete mixing is appropriate.

### 3.2 Mass Balance

The macroscopic mass conservation law applied to the reaction part of the reactor can be written as follows

$$\begin{aligned}\frac{dM_1(t)}{dt} &= \dot{M}_{in} + q_{in} \rho_f - \frac{q_{in}}{1 - g_{inter}} \rho_{inter}(t) \\ \frac{d}{dt} (V_1(t) \rho_1(t)) &= \dot{M}_{in} + q_{in} \rho_{in} - \frac{q_{in}}{1 - g_{inter}} \rho_{inter}(t)\end{aligned}\quad (19)$$

where  $\dot{M}_{in}$  is the mass input of FeSi,  $q_{in}$  is the volumetric inflow of leaching acid and  $\rho_1(t)$  and  $\rho_{inter}(t)$  are the slurry densities within the reaction region and in the outlet flow from the reaction region, respectively. Densities are a function of the solid's volume fraction, as given by

$$\rho_1(t) = \rho_f (1 - g_1(t)) + \rho_p g_1(t) \quad (20)$$

$$\rho_{inter}(t) = \rho_f (1 - g_{inter}(t)) + \rho_p g_{inter}(t). \quad (21)$$

In turn, the solid's volume fraction is a function of the third moment of the particle size distribution

$$g_1(t) = \frac{\pi}{6} \int_0^{D_p^{max}} D_p^3 \psi_1(D_p, t) dD_p \quad (22)$$

$$g_{inter}(t) = \frac{\pi}{6} \int_0^{D_p^{max}} D_p^3 \psi_{inter}(D_p, t) dD_p. \quad (23)$$

It must be noted that equation 19 assumes that the acid does not accumulate in the reaction region and that the outflow is thus composed of the acid inflow plus the fines displaced by the acid. This assumption is reasonable according to the operation of the industrial reactor, since the acid is fed continuously.

Now, the application of the macroscopic mass conservation law to the storage region of the reactor results in the following expressions

$$\begin{aligned}\frac{dM_2(t)}{dt} &= \frac{q_{in}}{1 - g_{inter}} \rho_{inter}(t) - q_{out,2}(t) \rho_2(t) \\ \frac{d}{dt} (V_2(t) \rho_2(t)) &= \frac{q_{in}}{1 - g_{inter}} \rho_{inter}(t) - q_{out,2}(t) \rho_2(t)\end{aligned}\quad (24)$$

where

$$\rho_2(t) = \rho_f (1 - g_2(t)) + \rho_p g_2(t) \quad (25)$$

$$g_2(t) = \frac{\pi}{6} \int_0^{D_p^{max}} D_p^3 \psi_1(D_p, t) dD_p. \quad (26)$$

and  $q_{out,2}(t)$  occurs by gravity and can be derived by applying Bernoulli's law between the surface of the liquid and the physical outlet, yielding to

$$q_{out,2} = C_D \frac{\pi}{4} D_{out}^2 \sqrt{2g \left( \frac{4}{\pi D_r^2} (V_1 + V_2 - V_{semiconical}) - h_{out} \right)} \quad (27)$$

where  $D_r$  is the diameter of the cylindrical part of the reactor,  $h_{\text{out}}$  is the distance between the bottom of the cylindrical part of the reactor and the outlet orifice,  $V_{\text{semiconical}}$  is the volume of the reactor that has semiconical shape,  $D_{\text{out}}$  is the diameter of the outlet orifice, and  $C_D$  is the coefficient of discharge, which typically has a value of 0.64 for liquids or slurries (Coulson & Richardson 1978).

### 3.3 Energy Balance

Temperature has an important influence on the disintegration of particles. This makes it necessary to use a nonisothermal model. In the model suggested here, we assume that the temperature is the same both in the reaction region and in the storage region of the reactor. Such an assumption is reasonable since the main heat input is provided by the acid inflow, and the corresponding flowrate is very high in comparison to the FeSi feed, causing great turbulence within the reactor and therefore good heat transmission, with the FeSi feed being heated to the reactor temperature almost instantly.

Therefore, the energy balance applied to the whole reactor is given by

$$\frac{dU(t)}{dt} = h_{\text{in}} - h_{\text{out}} - Q \quad (28)$$

where  $U(t)$  is the internal energy of the system,  $h_{\text{in}}$  and  $h_{\text{out}}$  are the enthalpy flow entering and leaving the reactor, respectively and  $Q$  is the heat loss to the surroundings. It must be noted that in the energy balance, the kinetic and the gravitational components of energy have been neglected in comparison to the internal energy component  $U(t)$ . Moreover, we assume that the internal energy and the enthalpies are functions of temperature, so that we can rewrite equation 28 as follows

$$\begin{aligned} \frac{d}{dt} \{V_1(t) \rho C_{p1}(t) (T(t) - T_{\text{ref}}) + V_2(t) \rho C_{p2}(t) (T(t) - T_{\text{ref}})\} = \\ C_{p_p}(T_s - T_{\text{ref}}) + q_{\text{in}} \rho_f C_{p_l}(T_{\text{in}} - T_{\text{ref}}) - q_{\text{out},2}(t) \rho C_{p2}(t) (T(t) - T_{\text{ref}}) \end{aligned} \quad (29)$$

where  $C_{p_p}$  and  $C_{p_l}$  are the heat capacities (kcal / kg K) of FeSi and the acid, respectively,  $T_s$  is the surroundings temperature (K),  $T_{\text{ref}}$  is the reference temperature (K) used to calculate enthalpies,  $\rho C_{p1}(t)$  and  $\rho C_{p2}(t)$  are the average heat capacity (kcal / m<sup>3</sup> K) of the slurry within the reaction region and within the storage region, respectively. The average heat capacities are functions of the solids volumetric fraction as shown below

$$\rho C_{p1}(t) = \rho_f C_{p_f} (1 - g_1(t)) + \rho_p C_{p_p} g_1(t) \quad (30)$$

$$\rho C_{p2}(t) = \rho_f C_{p_f} (1 - g_2(t)) + \rho_p C_{p_p} g_2(t). \quad (31)$$

### 3.4 Overview of the model

Table 1 summarizes the model, which consists of 1 integrodifferential equation, 4 implicit ordinary differential equations, 7 algebraic equations and 3 integral equations.

### 3.5 Discretization of the model

Integrodifferential equations are very difficult to solve. The method of moments, as developed by Hulburt & Katz (1964) (Hulburt & Katz 1964), is the most widely used method

Table 1: Overview of the Model

$\frac{d\psi_1(D_p, t)}{dt} + \frac{\psi_1(D_p, t)}{V_1(t)} \frac{dV_1(t)}{dt} = \frac{1}{V_1(t)} \left( \dot{M}_{\text{in}}(t) f_{\text{in}}(D_p, t) - \frac{q_{\text{in}}}{1 - g_{\text{inter}}(t)} \psi_{\text{inter}}(D_p, t) \right) + \int_{D_p}^{\infty} b(D_p, y) \eta(D_p, y) a(D_p, T) \psi_1(y, t) dy - a(D_p, T) \psi_1(D_p, t)$
<p>where <math>a(D_p, T) = \frac{k_a \exp(k_T T)}{D_p^n}</math></p>
<p>and <math>b\eta(D_p, y) = A_1 \exp\left(-\beta_1 \left(1 - \frac{D_p}{D_p^*}\right)^2\right) + \frac{A_2}{D_p} \exp\left(-\beta_2 \log^2\left(1 - \frac{D_p y}{(y - D_p) D_p^*}\right)\right) \frac{y^3}{D_p^3}</math></p>
$\psi_{\text{inter}}(D_p, t) = \begin{cases} \psi_1(D_p, t) & \text{for } D_p \leq D_{\text{cut}} \\ 0 & \text{for } D_p > D_{\text{cut}} \end{cases}$
$D_{\text{cut}} = 0.33 \frac{\rho_f}{g_r (\rho_p - \rho_f)} \left( \frac{u_{et}}{(1 - g_2(t))^n} \right)^2$
$\frac{d}{dt} (V_1(t) \rho_1(t)) = \dot{M}_{\text{in}} + q_{\text{in}} \rho_{\text{in}} - \frac{q_{\text{in}}}{1 - g_{\text{out},1}(t)} \rho_{\text{inter}}(t)$
$\rho_1(t) = \rho_f (1 - g_1(t)) + \rho_p g_1(t)$
$\rho_{\text{inter}}(t) = \rho_f (1 - g_{\text{inter}}(t)) + \rho_p g_{\text{inter}}(t)$
$g_1(t) = \frac{\pi}{6} \int_0^{D_p^{\text{max}}} D_p^3 \psi_1(D_p, t) dD_p$
$g_{\text{inter}}(t) = \frac{\pi}{6} \int_0^{D_p^{\text{max}}} D_p^3 \psi_{\text{inter}}(D_p, t) dD_p$
$\frac{d\psi_2(D_p, t)}{dt} + \frac{\psi_2(D_p, t)}{V_2(t)} \frac{dV_2(t)}{dt} = \frac{1}{V_2(t)} \left( \frac{q_{\text{in}}}{1 - g_{\text{inter}}(t)} \psi_{\text{inter}}(D_p, t) - q_{\text{out}}(t) \psi_2(D_p, t) \right)$
$q_{\text{out}}(t) = C_D \frac{\pi}{4} D_{\text{out}}^2 \sqrt{2g \left( \frac{4}{\pi D_r^2} (V_1(t) + V_2(t) - V_{\text{semiconical}}) - h_{\text{out}} \right)}$
$\frac{d}{dt} (V_2(t) \rho_2(t)) = \frac{q_{\text{in}}}{1 - g_{\text{inter}}} \rho_{\text{inter}}(t) - q_{\text{out}}(t) \rho_2(t)$
$\rho_2(t) = \rho_f (1 - g_2(t)) + \rho_p g_2(t)$
$g_2(t) = \frac{\pi}{6} \int_0^{D_p^{\text{max}}} D_p^3 \psi_1(D_p, t) dD_p$
$\frac{d}{dt} \{V_1(t) \rho C_{p1}(t) (T(t) - T_{\text{ref}}) + V_2(t) \rho C_{p2}(t) (T(t) - T_{\text{ref}})\} = \dot{M}_{\text{in}} C_{pp} (T_s - T_{\text{ref}}) + q_{\text{in}} \rho_f C_{pl} (T_{\text{in}} - T_{\text{ref}}) - q_{\text{out}}(t) \rho C_{p2}(t) (T(t) - T_{\text{ref}}) - Q$
$\rho C_{p1}(t) = \rho_f C_{pf} (1 - g_1(t)) + \rho_p C_{pp} g_1(t)$
$\rho C_{p2}(t) = \rho_f C_{pf} (1 - g_2(t)) + \rho_p C_{pp} g_2(t)$

to reduce integro-differential equations into a set of ordinary equations, but it is not applicable here because this would lead to an open set of equations.

Examples of numerical solution methods proposed in the literature (Ramkrishna 1985) are: the method of weighted residuals, the method of self-preserving distributions, Monte Carlo simulation techniques, the size interval-by-size marching method and discretization via fixed/moving pivot techniques. Of the numerical methods, those based on discretization of the continuous PBE are reported to be the most attractive from the computational point of view (Kumar & Ramkrishna 1996).

Discretization techniques aim at the formulation of PBE in discrete particle size space. This is done by integrating the continuous PBE equation over a discrete size interval, say  $D_{p,i}$  to  $D_{p,i+1}$ ,

$$\begin{aligned} \int_{D_{p,i}}^{D_{p,i+1}} \frac{1}{V} \frac{\partial(V\psi)}{\partial t} dD_p &= \int_{D_{p,i}}^{D_{p,i+1}} \frac{1}{V} (Q_{\text{in}}\psi_{\text{in}} - Q\psi) dD_p - \int_{D_{p,i}}^{D_{p,i+1}} a(D_p)\psi(D_p, t) dD_p \\ &+ \int_{D_{p,i}}^{D_{p,i+1}} \int_{D_p}^{D_{p,\text{max}}} b(D_p, y) a(y)\psi(y, t) dy dD_p, \end{aligned} \quad (32)$$

where the discrete particle size distribution,  $\phi_i(t)$  is given by

$$\phi_i(t) = \int_{D_{p,i}}^{D_{p,i+1}} \psi(D_p, t) dD_p, \quad (33)$$

and the number of intervals used to represent the total population of particles is  $N$ . Thus,  $i = 1, 2, \dots, N$ . The various discretization methods differ in the way of relating the continuous and discrete particle-size density distribution,  $\psi(D_p, t)$  and  $\phi_i(t)$ .

The main disadvantage of discretization methods is that the discretized model may not be consistent with the number and mass conservation laws, or any other integral property of interest associated to the entire population. Often, the accuracy of the solutions is improved by using finer discretization grids, but this is incurring a very high computational costs. The method proposed by Kumar and Ramkrishna (1996) (Kumar & Ramkrishna 1996) improves considerably the effectiveness of discretization. They suggest that the discrete equations are internally consistent with regard to the desired moments of interest of the distribution, thus ensuring the preservation of the quantities of interest, while relaxing the accuracy of other less important quantities.

The numerical technique divides the entire size range into small sections. The size range contained in between two sizes  $D_{p,i}$  and  $D_{p,i+1}$  is called the  $i$ th section. The particle population in this range is represented by a size  $x_i$ , such that  $D_{p,i} < x_i < D_{p,i+1}$ . This technique allows for the use of a general grid, for example, fine in some ranges and coarse elsewhere. The particle population is assumed to be concentrated at representative sizes,  $x_i$ 's, having a zero value for other sizes. Hence, the continuous and the discrete particle size density distribution,  $\psi(D_p, t)$  and  $\phi_i(t)$ , are related as follows

$$\psi(D_p, t) = \sum_{i=1}^N \phi_i(t) \delta(D_p - x_i) \quad (34)$$

where  $\delta(D_p - x_i)$  is the Delta Dirac function. Once this method is applied to the system under study we obtain the discretized model shown in Table 2. The discretized system of equations is thus an implicit nonlinear Differential/Algebraic equation (DAE) system.

Table 2: Discretized model

$\frac{d\phi_{1,i}(t)}{dt} + \frac{\phi_{1,i}(t)}{V_1(t)} \frac{dV_1(t)}{dt} = \frac{1}{V_1(t)} \left( \dot{M}_{in}(t) F_{in}(t) - \frac{q_{in}}{1 - g_{inter}(t)} \phi_{inter,i}(t) \right)$ $+ \sum_{k>i}^N n_{i,k} a_k \phi_k(t) - a_i \phi_i(t)$
<p>where <math>i = 1, 2, \dots, N</math>,</p> $n_{i,k} = \int_{x_i}^{x_{i+1}} \left( \frac{x_{i+1}^3 - D_p^3}{x_{i+1}^3 - x_i^3} \right) b\eta(D_p, x_k) dD_p + \int_{x_{i-1}}^{x_i} \left( \frac{D_p^3 - x_{i-1}^3}{x_i^3 - x_{i-1}^3} \right) b(D_p, x_k) dD_p,$ $b\eta(D_p, x_k) = \left( A_1 \exp \left( -\beta_1 \left( 1 - \frac{D_p}{D_p^*} \right)^2 \right) + \frac{A_2}{D_p} \exp \left( -\beta_2 \log^2 \left( 1 - \frac{D_p x_k}{(y - D_p) D_p^*} \right) \right) \right) \frac{y^3}{D_p^3}$ <p>and <math>a_k = \frac{k_a \exp(k_T T)}{x_k^n}</math></p>
$V_1(t) \frac{d\rho_1(t)}{dt} + \rho_1(t) \frac{dV_1(t)}{dt} = \dot{M}_{in} + q_{in} \rho_{in} - \frac{q_{in}}{1 - g_{out,1}(t)} \rho_{inter}$
$g_1(t) = \frac{\pi}{6} \sum_{i=1}^N x_i^3 \phi_{1,i}(t)$
$\rho_1(t) = \rho_f (1 - g_1(t)) + \rho_p g_1(t)$
$D_{cut} = 0.33 \frac{\rho_f}{g_r (\rho_p - \rho_f)} \left( \frac{u_{et}}{(1 - g_2(t))^n} \right)^2$
$\phi_{inter,i}(t) = \begin{cases} \phi_{1,i}(t) & \text{for } D_p \leq D_{cut} \\ 0 & \text{for } D_p > D_{cut} \end{cases}$
$g_{inter}(t) = \frac{\pi}{6} \sum_{i=1}^N x_i^3 \phi_{inter,i}(t)$
$\rho_{inter}(t) = \rho_f (1 - g_{inter}(t)) + \rho_p g_{inter}(t)$
$\frac{d\phi_{2,i}(t)}{dt} + \frac{\phi_{2,i}(t)}{V_2(t)} \frac{dV_2(t)}{dt} = \frac{1}{V_2(t)} \left( \frac{q_{in}}{1 - g_{inter}(t)} \phi_{inter,i}(t) - q_{out}(t) \phi_{2,i}(t) \right)$
$V_2(t) \frac{d\rho_2(t)}{dt} + \rho_2(t) \frac{dV_2(t)}{dt} = \frac{q_{in}}{1 - g_{inter,1}(t)} \rho_{inter}(t) - q_{out}(t) \rho_2(t)$
$q_{out}(t) = C_D \frac{\pi}{4} D_{out}^2 \sqrt{2g \left( \frac{4}{\pi D_r^2} (V_1(t) + V_2(t)) - V_{semiconical} \right) - h_{out}}$
$g_2(t) = \frac{\pi}{6} \sum_{i=1}^N x_i^3 \phi_{2,i}(t)$
$\rho_2(t) = \rho_f (1 - g_2(t)) + \rho_p g_2(t)$
$\frac{d}{dt} \{ V_1(t) \rho C_{p1}(t) (T(t) - T_{ref}) + V_2(t) \rho C_{p2}(t) (T(t) - T_{ref}) \} =$ $\dot{M}_{in} C_{pp} (T_s - T_{ref}) + q_{in} \rho_f C_{pf} (T_{in} - T_{ref}) - q_{out}(t) \rho C_{p2}(t) (T(t) - T_{ref}) - Q$
$\rho C_{p1}(t) = \rho_f C_{pf} (1 - g_1(t)) + \rho_p C_{pp} g_1(t)$
$\rho C_{p2}(t) = \rho_f C_{pf} (1 - g_2(t)) + \rho_p C_{pp} g_2(t)$

## 4 Analysis of the DAE

Historically, sets of DAEs were frequently restated and solved as ODEs, by differentiation and/or extensive algebraic manipulation, often destroying the natural structure of the system. Today, it is becoming more common to deal with such problems in their original, natural DAE form, mainly because the variables in the original DAE typically have some physical significance, whereas those that result after manipulation into an ODE may not (Lefkopoulos & Stadherr 1993). However, *differential and algebraic equations (DAEs) are not ordinary differential equations (ODEs)* (Petzold 1985). A number of difficulties can arise when numerical methods are used to solve systems of differential/algebraic equations of the form  $\mathbf{F}(t, \mathbf{y}, \mathbf{y}') = 0$ . These problems look much like standard ordinary differential equation (ODE) systems of the form  $\mathbf{y}' = \mathbf{f}(t, \mathbf{y})$  and, of course, include these systems as a special case. Many of the DAE systems can be solved using numerical methods which are commonly used for solving stiff systems of ODEs, such as backward differentiation formulas (BDF). Others can be solved using such methods but only after substantial modification to the strategies usually used in codes implementing those methods (Petzold 1985).

DAE systems can be characterized using the concept of *index*. The index can be thought of as a measure of the variation of the DAE structure from a standard ODE system (Lefkopoulos & Stadherr 1993). Therefore, the first thing to do when dealing with DAE systems is to determine its index.

First, let us define in more detail the concept of index of a DAE. It can be defined as the minimum number of times we must differentiate all or part of  $\mathbf{F}(t, \mathbf{y}, \mathbf{y}') = 0$  with respect to time  $t$  in order to determine  $\mathbf{y}'$  as a continuous function of  $\mathbf{y}$  and  $t$ . More formally, it can be stated that the index of a DAE is the smallest nonnegative integer  $\nu$  such that  $\mathbf{F}$  has  $\nu$  continuous derivatives and the nonlinear system:

$$\begin{aligned} \mathbf{F}(t, \mathbf{y}, \mathbf{y}') &= 0 \\ \frac{d\mathbf{F}}{dt}(t, \mathbf{y}, \mathbf{y}', \mathbf{y}'') &= \frac{d\mathbf{F}}{d\mathbf{y}}\mathbf{y}' + \frac{d\mathbf{F}}{d\mathbf{y}'}\mathbf{y}'' + \frac{\partial\mathbf{F}}{\partial t} = 0 \\ &\vdots \\ \frac{d^\nu\mathbf{F}}{dt^\nu}(t, \mathbf{y}, \mathbf{y}', \mathbf{y}'', \dots, \mathbf{y}^\nu, \mathbf{y}^{\nu+1}) &= 0 \end{aligned}$$

when viewed as relating  $t, \mathbf{y}, \mathbf{y}', \mathbf{y}'', \dots, \mathbf{y}^\nu, \mathbf{y}^{\nu+1}$  as independent variables, is solved for  $\mathbf{y}'$  uniquely in terms of  $\mathbf{y}$  and  $t$ , i.e. there is an underlying ODE  $\mathbf{y}' = \mathbf{y}'(z, t)$ . The definition implies that any pure ODE is an index-zero DAE, and a system of algebraic equations has an index of one provided it is nonsingular.

For the purposes of index analysis of a DAE it is often convenient to partition the equations  $\mathbf{F}$  into differential equations  $\mathbf{f}$  and algebraic equations  $\mathbf{g}$ . Thus, without loss of generality, the DAE can be rewritten as follows

$$\begin{aligned} \mathbf{f}(t, \mathbf{y}, \mathbf{y}') &= 0 \\ \mathbf{g}(t, \mathbf{y}) &= 0. \end{aligned}$$

It can be shown that the DAE has an index of one if and only if the matrix

$$B = \begin{pmatrix} \frac{d\mathbf{f}}{d\mathbf{y}'} \\ \frac{d\mathbf{g}}{d\mathbf{y}} \end{pmatrix} \quad (35)$$

is nonsingular (Lefkopoulos & Stadherr 1993).

If we apply the criteria in equation 35 to our DAE system, we obtain a matrix that is a function of  $t$  and of the internal vector  $\mathbf{y}$ . Therefore, the index of the DAE system may vary during integration. It can be proved that the DAE under study is index-one as long as the volume of slurry within the reaction region and within the storage region is distinct from zero, or what is the same, the model is an index-one implicit DAE except when the reactor is empty (i.e., during start-up). The advantage of index-1 systems is that they do not need reformulation in order to be solved.

Another difference between ODEs and DAEs is that in the latter we must specify consistent initial conditions, and this can become a challenging problem for certain DAEs. For a set of initial conditions to be consistent, it must satisfy the system at an initial time  $t_0$

$$\mathbf{F}(t_0, \mathbf{y}_0, \mathbf{y}'_0) = 0. \quad (36)$$

Note that the term “initial conditions” is used to refer to the vector  $(\mathbf{y}_0, \mathbf{y}'_0)$  rather than simply to  $\mathbf{y}_0$ . This is a necessary condition, but not always sufficient for consistency. Usually, some or all of the equations resulting from differentiating  $\mathbf{F}$   $\nu$  times with respect to time have to be satisfied too.

The most widely used approach to determination of consistent initial conditions is to reduce the system to an index-zero system. The system under study is index one, so in order to reduce the system to an index-zero system we have to differentiate the algebraic equations with respect to time once, as shown below

$$\frac{d\phi_{\text{inter},i}(t)}{dt} = \begin{cases} \frac{d\phi_i(t)}{dt} & \text{for } D_p \leq D_{\text{cut}} \\ 0 & \text{for } D_p > D_{\text{cut}} \end{cases} \quad (37)$$

$$\frac{dg_1(t)}{dt} = \frac{\pi}{6} \sum_{i=1}^N x_i^3 \frac{d\phi_{1,i}(t)}{dt} \quad (38)$$

$$\frac{d\rho_1(t)}{dt} = (\rho_p - \rho_f) \frac{dg_1(t)}{dt} \quad (39)$$

$$\frac{dD_{\text{cut}}(t)}{dt} = 2n \cdot 0.33 \frac{\rho_f}{g_r (\rho_p - \rho_f)} \frac{u_{\text{et}}^2}{(1 - g_2(t))^{2n+1}} \frac{dg_2(t)}{dt} \quad (40)$$

$$\frac{dg_{\text{inter}}(t)}{dt} = \frac{\pi}{6} \sum_{i=1}^N x_i^3 \frac{d\phi_{\text{inter},i}(t)}{dt} \quad (41)$$

$$\frac{d\rho_{\text{inter}}(t)}{dt} = (\rho_p - \rho_f) \frac{dg_{\text{inter}}(t)}{dt} \quad (42)$$

$$\frac{dq_{\text{out}}(t)}{dt} = \frac{C_D \sqrt{\pi} g_r D_{\text{out}}^2}{D_r} \frac{1}{\sqrt{(4V_1(t) + 4V_2(t) - 4V_{\text{semiconical}} - h_{\text{out}} \pi D_r^2)}} \quad (43)$$

$$\left( \frac{dV_1(t)}{dt} + \frac{dV_2(t)}{dt} \right) \quad (44)$$

$$\frac{dg_2(t)}{dt} = \frac{\pi}{6} \sum_{i=1}^N x_i^3 \frac{d\phi_{2,i}(t)}{dt} \quad (45)$$

$$\frac{d\rho_2(t)}{dt} = (\rho_p - \rho_f) \frac{dg_2(t)}{dt} \quad (46)$$

$$\frac{d\rho C_{p1}(t)}{dt} = (\rho_p C_{p_p} - \rho_f C_{p_f}) \frac{dg_1(t)}{dt} \quad (47)$$

$$\frac{d\rho C_{p2}(t)}{dt} = (\rho_p C_{p_p} - \rho_f C_{p_f}) \frac{dg_2(t)}{dt} \quad (48)$$

Now, we can arbitrarily decide the initial value for the differential variables of the DAE, i.e.  $\phi_{1,i}(t)$ ,  $V_1(t)$ ,  $\phi_{2,i}(t)$ ,  $V_2(t)$  and  $T(t)$ . Once this is done, the remaining initial conditions are calculated by solving the system of equations composed by the equations in Table 2 and equations 37 to 48 evaluated at  $t = 0$ . It must be noted that in the case under study some of the initial conditions can be calculated by direct substitution in the equations, but others result from the solution of a linear system of equations. By following this approach, we get a set of consistent initial conditions  $(\mathbf{y}_0, \mathbf{y}'_0)$ .

It is useful to discuss in more detail the selection of the degrees of freedom.  $V_1(0)$ ,  $V_2(0)$  and  $T(0)$  can be chosen making use of the knowledge of the operation of the reactor. However, to select the *discrete number-density* particle size distribution functions per unit working volume,  $\phi_{1,i}(t)$  and  $\phi_{2,i}(t)$ , is not straightforward. One possible approach, that is applied here, is the following:

1. Choose a continuous weight-density particle size distribution.
2. Apply the discretization grid and integrate in order to calculate the discrete weight-density particle size distribution
3. Transform the distribution from weight-basis to number-basis.

Initially, B-splines were used to fit a possible continuous weight-density particle size distribution. B-splines were chosen because they usually give a good fitting to data, they allow interpolation and can be easily integrated. Matlab has routines to interpolate, evaluate and integrate B-splines. However, this approach was not very succesful because the interpolation between points can yield negative values for those regions of the distribution function close to zero. Negative values do not have physical meaning in this context. Therefore, this approach was rejected. Instead, it was decided to use a log-normal distribution function for the initial weight-based distribution function. The log-normal distribution is often used in the empirical representation of particle size distributions (Randolph & Larson 1988). The variant used here can be used for distributions that are truncated

below a minimum size and/or above a maximum size, and is written as follows

$$f = \frac{1}{(2\pi)^{0.5} \log \sigma} \exp \left\{ -\log \left( \frac{(D_p - D_{p,\min})(D_{p,\max} - D_{p,\min})}{(D_{p,\max} - D_{p,\min}) \bar{D}_p 2^{0.5} \log \sigma} \right)^2 \right\} \quad (49)$$

where  $D_{p,\min}$  is the minimum diameter,  $D_{p,\max}$  is the maximum diameter,  $\bar{D}_p$  is the average diameter and  $\sigma$  is the standard deviation.

Finally, one issue that arised in this problem is the need of scaling the states and the system of equations. The variables of the system show a wide range. Hence, the discrete number-density particle can have a value in the order of  $10^9$ , whereas the cut-size diameter can have a value of the order of  $10^{-3}$ . Such a large difference in order of magnitude can cause ill-conditioning problems when calculating the Jacobian of the system of equations. In order to avoid such problems, the system of equations was rewritten in terms of scaled variables and the equations themselves were also scaled. In both cases, the scaling factor was the initial value of the variables except for those variables whose value is 0.

Once the DAE has been categorised by its index, and consistent initial conditions have been calculated, we are in a condition to select the method of solution for the DAE system. Linear Multistep methods, and more precisely, the Backward Differentiation Formulas (BDF), have emerged as the most popular method to solve DAEs. The simplest first order BDF method is the implicit Euler method, which consists of replacing the derivative in  $\mathbf{F}(t, \mathbf{y}, \mathbf{y}') = 0$  by a backward difference

$$\mathbf{F}(t_n, \mathbf{y}_n, \frac{\mathbf{y}_n - \mathbf{y}_{n-1}}{h}) = 0 \quad (50)$$

where  $h = t_n - t_{n-1}$ . The resulting system of nonlinear equations for  $\mathbf{y}_n$  at each time step is then usually solved by Newton's method (Brenan, Campbell & Petzold 1996). The  $k$ -step (constant stepsize) BDF consists of replacing  $\mathbf{y}'$  by the derivative of the polynomial which interpolates the computed solution at  $k + 1$  times  $t_n, t_{n-1}, \dots, t_{n-k}$ , evaluated at  $t_n$ . This yields

$$\mathbf{F}(t_n, \mathbf{y}_n, \frac{\rho \mathbf{y}_n}{h}) = 0 \quad (51)$$

where  $\rho \mathbf{y}_n = \sum \alpha_i \mathbf{y}_{n-i}$  and  $\alpha_i, i = 1, 2, \dots, k$  are the coefficients of the BDF method.

It is convenient to discuss the convergence of BDF method applied to fully-implicit index-one systems.

**Theorem 1 (Brenan et al. 1996)** *Let  $\mathbf{F}(t, \mathbf{y}, \mathbf{y}') = 0$  a uniform index one DAE on an interval  $I = [t_0, t_0 + T]$ . Then the numerical solution of  $\mathbf{F}(t, \mathbf{y}, \mathbf{y}') = 0$  by the  $k$ -step BDF with fixed stepsize  $h$  for  $k < 7$  converges to  $O(h^k)$  if all initial values are correct to  $O(h^k)$  accuracy and if the Newton iteration on each step is solved to  $O(h^{k+1})$  accuracy.*

Thus we can conclude that the DAE under study can be solved with a code based on the BDF method. Popular DAE solution codes based on BDFs are DASSL (Brenan et al. 1996) and LSODI (Brenan et al. 1996). Here, the `ode15s` code of the MATLAB ODE suite is used. It was chosen because MATLAB is one of the most widely used problem-solving environments. The `ode15s` code is based on a variant of the BDFs called numerical differentiation formulas (NDFs). For further information about `ode15s`, see (Shampine, Reichelt & Kierzenka 1999).

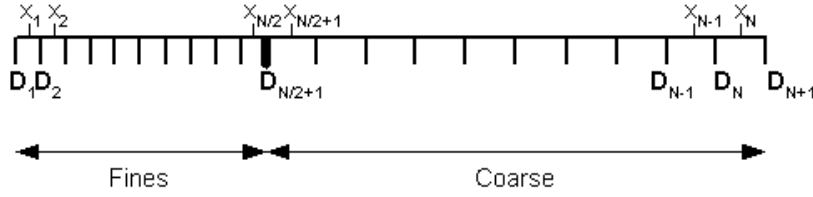


Figure 4: Discretization Grid

## 5 Simulation Results

The discretization grid was selected taking into account the operation of the reactor and the regions of interest in the particle size spectra. For example, it is advisable to have a fine grid in the region corresponding to the particles leaving the reactor. For this reason, the grid was divided into two regions: fine particles, corresponding to the sizes of particles leaving the reactor, and coarse particles. The total number of intervals are thus split in two, half of the intervals corresponding to the region of fines and half of the intervals corresponding to the region of coarse particles. Finally, a linear grid is used in both regions. Figure 4 shows a sketch of such a discretization grid. The number of intervals in the grid has been chosen by running simulations for different number of intervals and selecting the minimum number of intervals that provides the same results as finer grids, based on visual inspection of the results.

Simulations have been carried out with initial conditions and inputs in the range of values of the real reactor. The system is simulated until it reaches steady-state as regards PSD and then the response of the system to a step change in one of the inputs is simulated.

Figures 5, 6 and 7 shows the step response to a change in the FeSi feed from the normal operation feed rate to zero. It can be seen that the volume of the reaction region  $V_1(t)$  increases and never reached steady-state, since more FeSi is fed than consumed in the disintegration. Once the FeSi mass input is halved, the volume in the reaction region continue increasing, but a slower pace, as it could be expected. The volume of the storage region  $V_1(t)$  decreased, but again decreased at a slower pace after the step change. The change also affects the solid's particle fractions in both regions, decreasing in both cases, which is logical since less solid material is fed to the system whereas the fluid feed remains constant. Figure 6 shows that the step change in the FeSi feed  $\dot{M}_{in}$  results in an increase in Temperature  $T(t)$ , and this result is reasonable since the heat exchange between the cold FeSi feed and the hot acid flowrate has been reduced. The cut size  $D_c(t)$  is not very affected since the porosity in the storage region ( $1 - g_2(t)$ ) has not been modified to a large extent. Finally, Figure 7 indicates that the PSDs in the reactive region (RI), in the interflow between regions and in the storage region (RII) are not affected by a change in FeSi feedrate, as could be expected. It must be noted that the PSD in the storage area differs greatly from the PSD in the reaction area, as we expected. In the reaction area coarse particles predominate, whereas in the storage area only fines are present.

Let us take a look now at the simulations of a step change in the temperature of the acid flow, that is decreased by 10% with respect to the normal operating temperature.

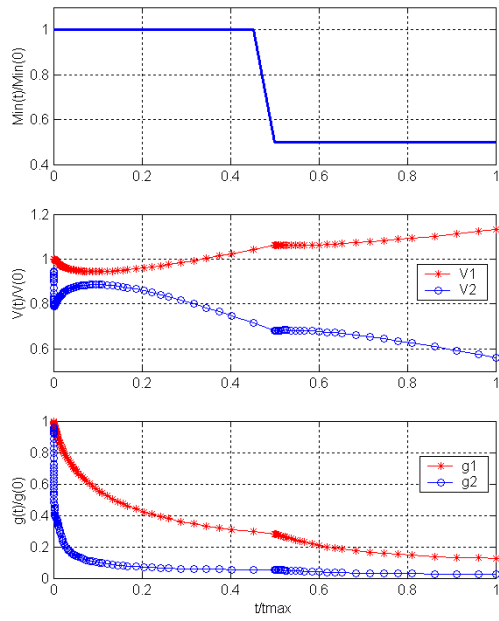


Figure 5: Step response to a change in FeSi feedrate.

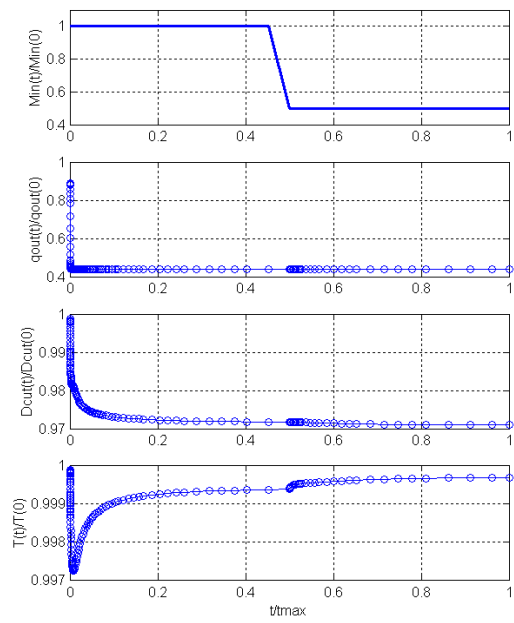


Figure 6: Step response to a change in FeSi feedrate.

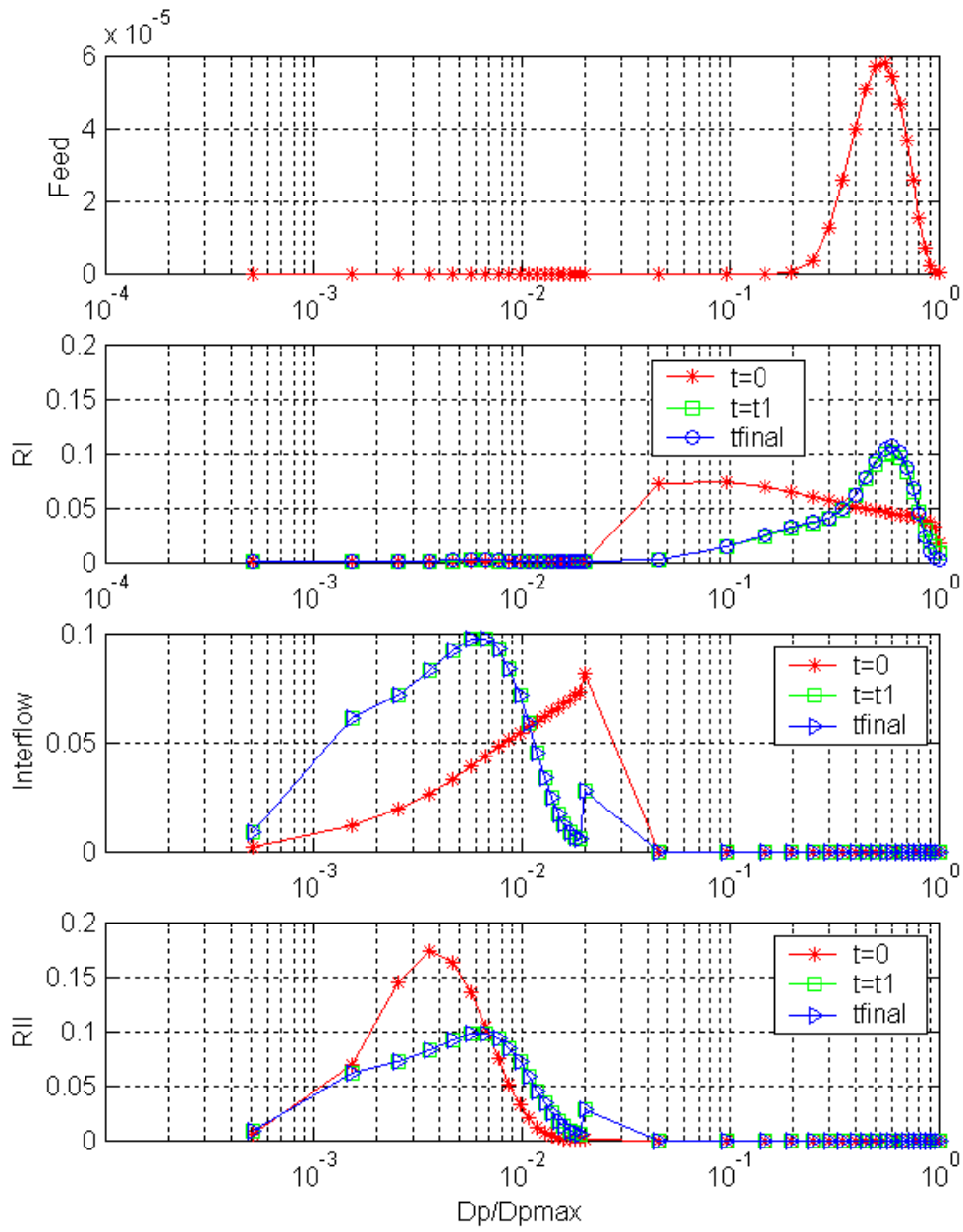


Figure 7: Step response to a change in FeSi feedrate.

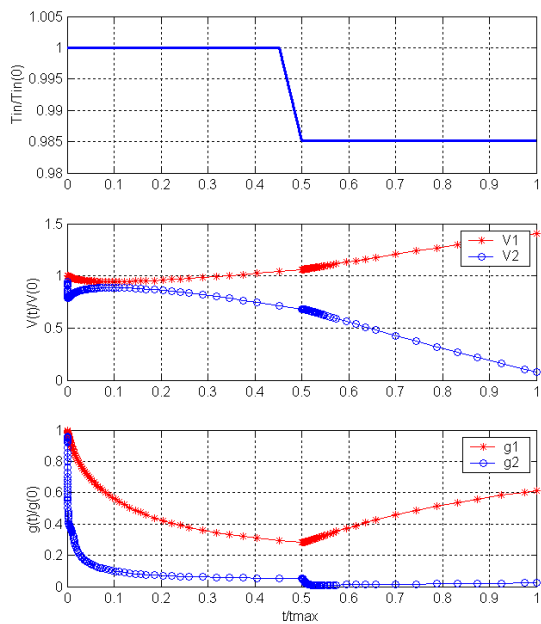


Figure 8: Step response to a change in acid temperature.

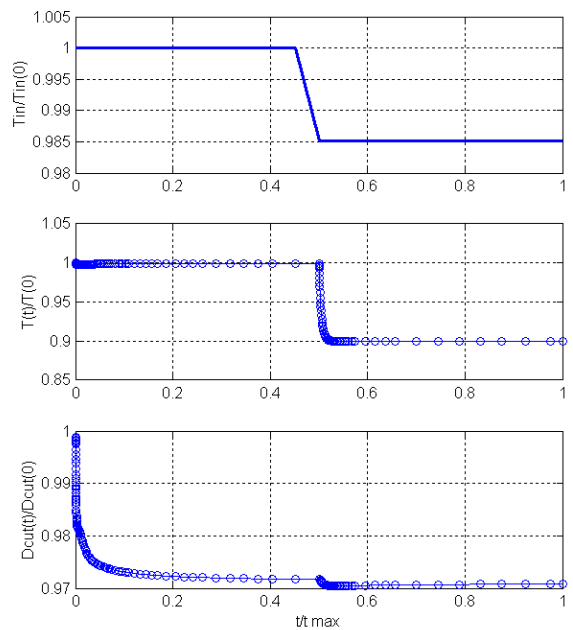


Figure 9: Step response to a change in acid temperature.

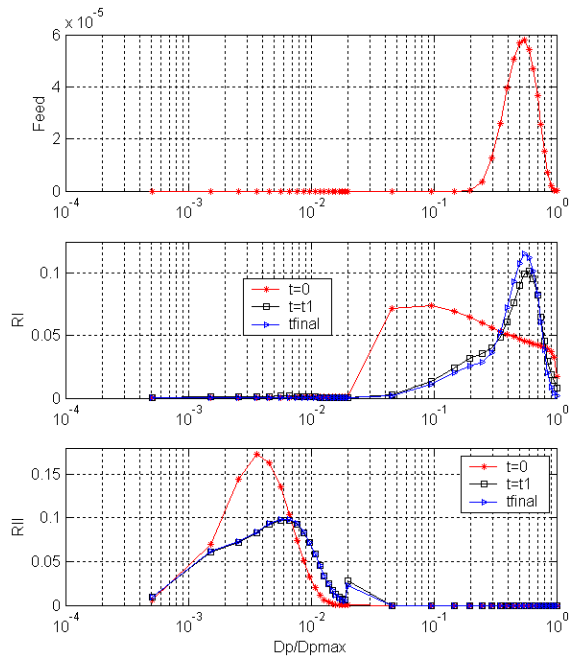


Figure 10: Step response to a change in acid temperature.

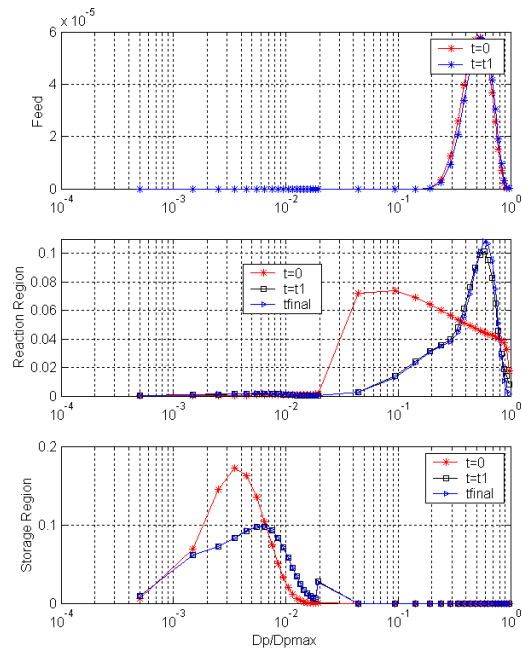


Figure 11: Step response to a change in the average diameter of FeSi feed.

The results are shown in Figures 8 and 9. As it can be observed in Figure 8, a drop in the acid temperature makes the disintegration to proceed more slowly. This means that FeSi accumulates in the reaction region and for this reason an increase of volume in this region is observed. In contrast, the volume of the storage region decreases due to the inhibition of fine production. The same reasoning explains the observed trends for the solid's volume fraction within the two regions. Figure 9 shows that an equivalent drop in the reactor temperature is obtained and that the cut diameter decreases because of the variation in the porosity of the storage region. The displacement of the PSD within the reaction area towards larger sizes and the change in PSD shape, observed in Figure 10, confirms that a drop in acid temperature hinders disintegration.

Figure 11 shows the result of a step change in the average size diameter of the FeSi feed. As it can be noticed, if coarser material is fed to the reactor, the PSD within the reaction region will experience a displacement towards larger sizes. In contrast to the response to a step change in temperature, the shape of PSD is now not modified, only displaced towards larger particle size.

The simulation results are satisfactory and seems to match qualitatively with the knowledge of the operation of the reactor. The new model resembles more closely to the behavior of the industrial reactor than the previous model.

## 6 Conclusions

The intention of this paper is to improve an existing dynamic model of the main reactor in the Silgrain<sup>®</sup> process for the production of Si from FeSi in order to resemble more closely the behavior of the real reactor. This requires the consideration of the momentum balance over the particles, since only the disintegrated material is displaced out from the reactor by the acid upflow, whereas the coarse material remains within the reactor until its disintegration. Furthermore, the energy balance has to be included since temperature plays an important role in the disintegration. Finally, a model for the disintegration terms based on laboratory experiments has been used.

The extended model consists of 1 integrodifferential equation, 4 implicit ordinary differential equations, 7 algebraic equations and 3 integral equations. The solution of such a difficult system of equations is approached here by using the discretization method proposed by Kumar and Ramkrishna (1996). The discretized system turns out to be a DAE system. DAEs are not ODEs and difficulties can be encountered when using numerical methods to solve them. Thus, DAEs require analysis and characterization and may require reformulation before considering its numerical solution. Such analysis is carried out here. It is concluded that the index of the system may vary with time and the operating conditions, but that for the normal range of operating conditions the DAE is implicit index-one and no reformulation is necessary. Attention is also given to the determination of consistent initial conditions since this is a key issue when solving DAEs. Particularly challenging is the selection of initial values for the *discrete number-density* particle size distribution functions per unit working volume. The need of scaling the state variables and the system equations is also discussed. The analysis of the DAE system concludes with the selection of a numerical method to solve the system. A method based on the BDFs is appropriate for this system and the the `ode15s` code of the MATLAB ODE suite,

which is based on a on a variant of the BDFs called Numerical Differentiation formulas (NDFs), is selected here.

The model is thus implemented in MATLAB and a simulation analysis is carried out to test the model. The simulation results are satisfactory and seem to match qualitatively with the known operation of the reactor.

To sum up, the main contributions of this paper refer to the following research areas:

- The use of the macroscopic population equation for modeling particulate processes. Previous researchers have made use of the assumption of complete-mixing for the particle size distribution. We make a more general use of the macroscopic population equation. The outflow PSD is not longer assumed to be equal to the PSD within the reactor, but both PSDs are related by considering the momentum balance over the particles. Another contribution in the modeling area is the suggested functions for the disintegration terms, which have been obtained after experimental results at laboratory scale.
- The use and solution of DAE systems. DAEs are challenging and require a more thorough analysis than other mathematical systems. Here we present a complete example of an analysis of a DAE system. The determination of the index of the system, of consistent initial conditions and of the method of solution were the main issues in the analysis.

Further work will include a comparison of the simulation results with experimental data from the industrial reactor. Also, the model is expected to be used to design advanced control systems which may lead to an improvement in the operation and yield of the reactor. Passivity-based control and predictive control are two of the model-based control techniques in which the model presented here could be used.

## Acknowledgments

The authors would like to thank Prof. Lorentz T. Biegler (Carnegie Mellon University, Pittsburgh, USA) for his useful advice regarding numerical solution of the model. We also want to acknowledge the help we received from Birte Skofteland, Anne Grete Forwald, Einar Andersen and the other employees at Elkem's Research Centre (Kristiansand, Norway) during the laboratory work that was carried out in this centre. The work of Marta Dueñas Díez is financially supported by the Research Council of Norway (project number 142994/432). Additional support has been obtained from Elkem ASA in relation to the case study.

## Notation

### Roman Symbols

Symbol	Definition	Units
$a(D_p, T)$	Particle breakup frequency function	$\text{min}^{-1}$
$b(D_p, y)$	Birth probability distribution function	$\text{m}^{-1}$
$B$	Particle birth rate	$1/\text{min m}^4$
$C_p$	Heat Capacity	$\text{kcal} / \text{kg K}$
$D$	Particle death rate	$1/\text{min m}^4$
$D_{\text{cut}}$	Cut size	$\text{m}$
$D_p$	Particle diameter	$\text{m}$
$f$	PSD as mass probability distribution function	$\text{m}^{-1}$
$g$	solid's volume fraction	-
$g_r$	Gravity acceleration	$\text{m} / \text{s}^2$
$N$	Number of intervals	-
$\dot{M}$	Mass Flowrate	$\text{kg} / \text{s}$
$q$	Volumetric slurry flow rate	$\text{m}^3 / \text{s}$
$Q$	Heat loss to the surroundings	$\text{kcal} / \text{min}$
$t$	Time	$\text{s}$
$T$	Temperature	$\text{K}$
$u_{et}$	Superficial velocity	$\text{m} / \text{s}$
$u_o$	Actual fluid velocity	$\text{m} / \text{s}$
$V$	Working volume of the reactor	$\text{m}^3$
$x$	Representative diameter	$\text{m}$
$y$	Mother particle diameter	$\text{m}$

### Greek Symbols

Symbol	Definition	Units
$\delta$	Delta Dirac function	-
$\eta$	Average number of daughter particles	-
$\rho$	Density	$\text{kg} / \text{m}^3$
$\rho C_p$	Volumetric Heat Capacity	$\text{kcal} / \text{m}^3 \text{K}$
$\phi$	discrete particle size number-density distribution	$\text{m}^{-3}$
$\psi$	continuous particle size number-density distribution	$\text{m}^{-4}$

### Abbreviations

BDF	Backward Differentiation Formulas
DAE	Differential and Algebraic Equations
NDF	Numerical Differentiation Formulas
ODE	Ordinary Differential Equations
PBE	Population Balance Equation
PSD	Particle Size Distribution

## Subscripts

Symbol	Definition
in	Relative to the inlet to the reactor
inter	Relative to the flow from the reaction to the storage region
max	maximum
min	minimum
$f$	Relative to the liquid
$p$	Relative to particle
out	Relative to the outflow from the reactor
1	Relative to the reaction region of the reactor
2	Relative to the storage region of the reactor

## References

- Aas, H. (1971), The silgrain process: Silicon metal from 90% ferrosilicon, *in* ‘Light Metals 1971: Proceedings of Symposia 100th AIME Annual Meeting’, number A71-47, pp. 650–667.
- Brenan, K. E., Campbell, S. L. & Petzold, L. R. (1996), *Numerical Solution of Initial-Value Problems in Differential-Algebraic Equations*, SIAM Society for Industrial and Applied Mathematics.
- Chen, Z., Prüss, J. & Warbecke, H. (1998), ‘A population balance model for disperse systems: Drop size distribution in emulsion’, *Chemical Engineering Science* **53**(5), 1059–1066.
- Coulson, J. & Richardson, J. (1978), *Chemical Engineering. Fluid Flow, Heat Transfer and Mass Transfer*, Vol. 1, Pergamon Press, Inc.
- Dueñas, M. & Lie, B. (2000), Modelling and simulation of a hydrometallurgical leaching reactor, *in* B. Elmegaard, N. Houbak, A. Jakobsen & F. J. Wagner, eds, ‘Proceedings SIMS 2000’, SIMS- Scandinavian Simulation Society and Technical University of Denmark, Lyngby (Denmark), pp. 199–225.
- Herbst, J. (1979), Rate processes in multiparticle metallurgical systems, *in* H. Sohn & M. Wadsworth, eds, ‘Rate Processes in Extractive Metallurgy’, Plenum Press, pp. 53–112.
- Herbst, J. & Asihene, S. (1993), Modelling and simulation of hydrometallurgical processes using the population balance approach, *in* V. Papangelakis & G. Demopoulos, eds, ‘Modelling, Simulation and Control of Hydrometallurgical Processes. Proceedings of the 32nd Annual Conference of Metallurgists of CIM’, Canadian Institute of Mining, metallurgy and petroleum, Quebec, pp. 3–44.
- Hulburt, H. M. & Katz, S. (1964), ‘Some problems in particle technology — A statistical mechanical formulation’, *Chemical Engineering Science* **19**, 555–574.

- Kapur, P. (1995), Particle population balance in granulation of iron ores by an auto-layering mode, *in* S. Mehrotra & R. Shekhar, eds, 'Mineral Processing. Recent Advances and Future Trends.', Allied Publishers ltd, pp. 703–717.
- Kumar, S. & Ramkrishna, D. (1996), 'On the solution of population balance equations by discretization — I. A fixed pivot technique', *Chemical Engineering Science* **51**(8), 1311–1332.
- Lefkopoulos, A. & Stadherr, M. A. (1993), 'Index analysis of unsteady-state chemical process systems — i. an algorithm for problem formulation', *Computers Chem. Engng.* **17**(4), 399–413.
- Margarido, F., Martins, J. P., Figueiredo, M. O. & Bastos, M. H. (1993), 'Kinetics of acid leaching refining of an industrial fe-si alloy', *Hydrometallurgy* **34**, 1–11.
- Petzold, L. R. (1985), 'Differential-algebraic equations are not ODEs', *SIAM J. Sci. Stat. Compt.* **3**(3), 49–95.
- Ramkrishna, D. (1985), 'The status of population balances', *Reviews in Chemical Engineering* **3**, 49–95.
- Randolph, A. (1964), 'A population balance for countable entities', *The Canadian Journal of Chemical engineering* **42**, 280–281.
- Randolph, A. D. & Larson, M. A. (1988), *Theory of Particulate Processes. Analysis and Techniques of Continuous Crystallization*, second edn, Academic Press, Inc.
- Rubisov, D. H. & Papangelakis, V. G. (1996*a*), 'Mathematical modelling of the transient behaviour of CSTRs with reactive particulates: Part 1— The population balance framework', *The Canadian Journal of Chemical Engineering* **74**, 353–362.
- Rubisov, D. H. & Papangelakis, V. G. (1996*b*), 'Mathematical modelling of the transient behaviour of CSTRs with reactive particulates: Part 2 — Application to pyrite pressure oxidation', *The Canadian Journal of Chemical Engineering* **74**, 363–371.
- Rubisov, D. & Papangelakis, V. (1995), 'Model-based analysis of pressure oxidation autoclave behaviour during process upsets', *Hydrometallurgy* **39**, 377–389.
- Shampine, L. F., Reichelt, M. W. & Kierzenka, J. A. (1999), 'Solving index-1 DAEs in matlab and simulink', *SIAM Review* **41**(3), 538–552.